Clinical and Translational Imaging
https://doi.org/10.1007/s40336-024-00659-8

RESEARCH

The clinical predictive value of radiomic features from [^{68}Ga]Ga-PSMA-11 and [^{18}F]F-PSMA-1007 PET in patients with prostate cancer: a preliminary comparative study

Daniele Antonio Pizzuto[1] · Michele Guerreri[3] · Constantinos Zamboglou[2] · Luca Boldrini[1] · Roberto Gatta[3] · Maria R. Ruggiero[1,4] · Marco De Summa[1,4] · Carmelo Caldarella[1] · Salvatore Annunziata[1]

Received: 8 July 2024 / Accepted: 11 September 2024

Abstract

Purpose To perform a preliminary evaluation of the clinical predictive value of radiomics from [^{68}Ga]Ga-PSMA-11 PET and [^{18}F]F-PSMA-1007 PET Positron Emission Tomography (PET) images of primary/recurrent prostate cancer (PCa) patients.

Methods Institutional PCa patients undergoing a staging/restaging [^{68}Ga]Ga-PSMA-11 or an [^{18}F]F-PSMA-1007 PET/computed tomography (CT) in 2021–2022 were retrospectively selected. Prostate specific antigen (PSA), Gleason Score (GS), lymph node status (N) and distant metastases (M) were collected. Volume of interests (VOIs) were placed to contour abnormal PSMA PET findings within the prostatic gland/fossa suspected for PCa. One hundred thirty-three radiomic features of both PSMA PET radioligands were extracted from each VOI, to explore their predictive value for the above-mentioned clinical/histological data.

Results Among 42 patients retrospectively included, significant different Total Lesion PSMA volumes (TL-PSMA) were found between the low/intermediate and high GS subgroups if this feature derived from [^{18}F]F-PSMA-1007 PET images (Mann-Whitney Test, $p = 0.01$). TL-PSMA values were found significantly different between the two GS subgroups when the entire cohort of both [^{68}Ga]Ga-PSMA-11 and [^{18}F]F-PSMA-1007 was considered (Mann-Whitney test, $p = 0.004$). The *Minimum histogram gradient intensity* feature was found to significantly predict the N-status (Mann Whitney test, $p = 0.009$). No correlations were found between the radiomic features and PSA values or M-status.

Conclusion Prostate TL-PSMA and *Minimum histogram gradient intensity* features of [^{68}Ga]Ga-PSMA-11 PET and [^{18}F]F-PSMA-1007 PET are candidate for building predictors of both high GS and N status in patients with PCa. [^{18}F]F-PSMA-1007 PET-derived TL-PSMA seem to correlate better than [^{68}Ga]Ga-PSMA-11 with high GS.

Keywords Radiomics · PSMA · PET · Prostate cancer

Introduction

Positron emission tomography with prostate-specific membrane antigen radioligands (PSMA PET) validly supports the risk-stratification of patients in primary prostate cancer PCa before surgery and/or radiotherapy, as well as in systemic treatment by exclusion or detection of metastases [1–4]. In both primary tumor and biochemical recurrence (BCR) settings, the accuracy and diagnostic performance of [^{68}Ga]Ga-PSMA-11 PET was shown to be similarly accurate to the Magnetic Resonance (MR) in detecting and localizing PCa foci [5] and superior to PET with choline-derived radiopharmaceuticals in PCa patients [6, 7]. Another PSMA radioligand, i.e. [^{18}F]F-PSMA-1007 was introduced in the

✉ Daniele Antonio Pizzuto
dapizzuto@gmail.com

1 Department of Radiology and Radiotherapy, Fondazione Policlinico Universitario A. Gemelli IRCCS, Rome 00168, Italy

2 Department of Radiation Oncology, University of Freiburg, 79106 Freiburg, Germany

3 Department of Clinical and Experimental Sciences, University of Brescia, Brescia 25121, Italy

4 Medipass S.p.a., Servizio Integrativo, Fondazione Policlinico Universitario A. Gemelli IRCCS, Rome 00168, Italy

Published online: 30 September 2024

clinical management of PCa, by taking advantage of lower urinary excretion and lower positron range, that allows a better spatial resolution than Gallium-labelled PSMA. In a head-to-head comparison on the same PCa patients both PSMA radioligands seem to be similarly effective to detect all dominant primary lesions in a cohort of intermediate/high risk PCa patients at primary staging [8], as well as in a cohort of BCR patient [9].

The high throughput radiomics approach translates medical images into minable data by extracting many quantitative features, as well as describing the intensity, shape, and heterogeneity of targeted lesions. Recently, PSMA PET radiomics of prostate were suggested to predict high-risk pathological tumor features in primary PCa patients and the BCR before salvage radiotherapy better than clinical outcome model [10, 11]. The predictive value of extracted radiomic features comparing [^{68}Ga]Ga-PSMA-11 to [^{18}F]PSMA-1007 was still unexplored before introducing this approach in clinical practice. This study aimed to perform a preliminary retrospective evaluation of the predictive value of radiomic analysis from [^{68}Ga]Ga-PSMA-11 PET and [^{18}F]PSMA-1007 PET images of prostatic gland/fossa, using as reference standard the main available clinical data in PCa patients.

Methods

Patients

Patients with diagnosis of PCa who underwent [^{68}Ga]Ga-PSMA-11 (Ga-PSMA) or an [^{18}F]F-PSMA-1007 (F-PSMA) PET co-registered with computed tomography (CT) at Fondazione Policlinico Universitario A. Gemelli IRCCS (Rome, Italy) were selected from a previously collected database from January 2021 and December 2022 (Ethical Committee Protocol Number: 5641). Two clinical purposes were considered: - patients with newly diagnosed PCa after biopsy-based histological confirmation (staging); - BCR patients (restaging), with evidence of Prostate Specific Antigen (PSA) serum values > 0.2 ng/mL after Radical Prostatectomy (RP) or an increase of at least 2 ng/mL from the end of radiotherapy (restaging) [12]. Only PCa patient with abnormal PET findings, according to the EANM standardized reporting guidelines v1.0 for PSMA-PET [13], encompassing either prostatic gland for staging or the fossa for restaging after RP or primary radiotherapy, were included.

PSA and biopsy-based Gleason Score (GS) Grade Group were collected for each patient. Furthermore, the presence of lymph node metastases (N) and/or distant metastases (M) were assessed by clinical and morphological evaluation (by histological specimen when available, CT, MR or PET/CT), that served as reference standard. The retrospective use of data from clinical routine was performed according to institutional rules. All procedures performed were in accordance with the ethical standards defined by the 1964 Helsinki Declaration and its later amendments.

Table 1 Acquisition modalities and reconstruction algorithms for PET-CT scanners

	Siemens Biograph mCT	Siemens Biograph Vision V600
Low dose CT scan	120 kV, 40–50 mAs	120 kV, 40–50 mAs
PET time and modality	2 min per bed	continuous bed motion: 1–2 mm/sec
Image reconstruction	UltraHD-PET: line-of-response row-action maximum likelihood algorithm 3D OSEM reconstruction + PSF modeling + TOF (2 iterations, 21 subsets) (voxel size: 3.2 × 3.2 × 5 mm3)	UltraHD-PET: line-of-response row-action maximum likelihood algorithm 3D OSEM reconstruction + PSF modeling + TOF (4 iterations and 5 subsets) (voxel size of 1.8 × 1.8 × 5 mm3)

CT: computed tomography; HD: high definition; OSEM: ordered subset expectation maximization; PSF: point spread function; PET: positron emission tomography; TOF; time-of-flight

PET protocol and analysis

PSMA PET protocol

Two MBq/kg of [^{68}Ga]Ga-PSMA-11 were intravenously administered to the patient. About 60 min after the injection, a non-contrast enhanced whole body CT was performed, immediately before a whole-body skull-base-to thigh PET scan.

Four MBq/Kg of [^{18}F]F-PSMA-1007 were intravenously administrated. Ninety minutes after the injection a non-contrast enhanced whole body CT was performed, immediately before the PET acquisition. No recommendations were suggested to the patients for the scan preparation of both protocols.

The following PET/CT scanners were used: Siemens Biograph mCT; Siemens Biograph Vision V600. Images derived from both Siemens Biograph mCT and Siemens Biograph Vision V600 scanners were reconstructed by True-X time-of-flight (TOF) (ultraHD PET) iterative reconstruction algorithms. Different acquisition time and modalities between scanners were used, i.e., 2 min per bed for Biograph mCT and PET continuous bed motion (1–2 mm/sec) for Vision V600. Voxels' size was slightly different between the two scanners (Table 1). Both scanners were accredited to European Association of Nuclear Medicine (EANM) Research Ltd. (EARL) [14], which ensures the harmonization of PET/CT systems in [^{18}F] and [^{68}Ga] multicentre

PET/CT studies. This approach minimizes inter- and intra-institution variability.

Image contouring and feature extraction

Two experienced nuclear medicine physicians (DAP and SA) delineated Volume of Interests (VOIs) through a gradient-based threshold using a PET segmentation tool (LesionID, version 7.0.5 of MIM Encore, MIM Software Inc., Cleveland, OH, USA), to encompass suspected primary or recurrent tumors in prostatic gland or fossa, respectively. Only PSMA foci in categories 4 and 5, according to the PSMA Reporting and Data System criteria (PSMA-RADS) [13], were considered. Manual corrections were performed, when necessary, to avoid the inclusion of spill-over areas in VOIs, due to [^{68}Ga]Ga-PSMA-11 accumulation in the bladder.

The set of 133 radiomics features included a set of conventional PET parameters and the set of radiomics feature available LIFEx v7.4.0, an IBSI-compliant software for radiomics analysis [15, 16]. All the features were normalized with the z-score. The conventional PET parameters (non IBS-compliant) were:

- Maximum and mean Standardized Uptake Value (tSUVmax and tSUVmean) which indirectly estimates the maximum and mean values of [^{68}Ga]Ga-PSMA-11 and [^{18}F]F-PSMA-1007 concentration within the VOI by the normalization with the patient's body weight;
- PSMA Tumor Volume (PSMA-TV) which represents the volume involving all the [^{68}Ga]Ga-PSMA-11 or [^{18}F]F-PSMA-1007 counts with at least 40% of SUVmax value;
- Total Lesion PSMA (TL-PSMA), calculated as tSUVmean × PSMA-TV.

Additionally, a 2-cm spherical VOI was drawn on the liver to extract liver SUVmean (LivSUVmean) and its standard deviation (SUVSD) as estimates of background intensity and noise, respectively. Tumor-to-background ratio (TBR) and Signal-to-noise ratio (SNR) were calculated as follows: tSUVmax/LivSUVmean and tSUVmax/SUVSD, respectively. These ratios were introduced in the analysis to normalize the variability caused by the different scanners.

Voxels were all resampled to 1.65 × 1.65 × 5 mm (x, y and z, respectively) before the features extraction.

Statistical analysis

Systematic differences between both the features extracted from [^{68}Ga]Ga-PSMA-11 and [^{18}F]F-PSMA-1007 and from different PET scanners respectively, were investigated via a Mann-Whitney test, to explore the feasibility to build a combined model.

To assess the predictive effectiveness of both [^{68}Ga]Ga-PSMA-11 and [^{18}F]F-PSMA-1007-derived radiomic features in relation to the outcomes, PSA was treated as a continuous variable, while N and M were categorized as binary outcomes. The GS Grade Group was both dichotomized with values of 0 or 1 based on whether the GS was lower/equal to 7 or higher than 7 and as a categorical-ordinal feature with four groups as follows: 1 = GS of 6, 2 = GS of 7 (3 + 4), 3 = GS of 7 (4 + 3), and 4 = GS greater than or equal to 8.

A Mann-Whitney test or a Pearson correlation coefficient, for binary or numeric outcomes, respectively, was performed to assess which of the features extracted from the PET images had the strongest association with the outcome. The categorical-ordinal GS Grade Group was investigated by the Kruskal-Wallis test.

To address the multiple tests conducted and to factor in the substantial number of covariates among various features, a qualitative threshold of 0.01 was established for statistical significance.

Results

Demographics characteristics of the patients included in the study are listed in Table 2. Of a total of 42 patients retrospectively collected, 17 underwent a [^{68}Ga]Ga-PSMA PET (8/17 performed on a Siemens Biograph mCT and 9/17 on a Siemens Biograph Vision V600) and 25 patients a [^{18}F]F-PSMA PET (9/25 performed on a Siemens Biograph mCT and 16/25 on a Siemens Biograph Vision V600). 14/42 patients were referred to PSMA PET scan for staging and 28/42 for restaging.

Both PET conventional and radiomic features, extracted from [^{68}Ga]Ga-PSMA-11 and [^{18}F]F-PSMA-1007PET images showed no statistically significant differences. In other words, the features extracted from the two different radiopharmaceutical did not vary significantly according to their p-value, so opening to the possibility to a model that considers [^{68}Ga]Ga-PSMA-11 and [^{18}F]F-PSMA-1007 as a single radiopharmaceutical (Fig. 1). Similarly, the features extracted from different scanners were found not to significantly differ.

There were no significant correlations observed between any of the PET conventional and radiomic features and the PSA values. These findings were consistent across all groups of subjects included in the analysis (TL-PSMA with Combined Pearson correlation test (PCC) = 0.38, SUVmax with PCC = 0.33,TBR with PCC = 0.32) (Fig. 2).

Table 2 Basic and clinical characteristics

	$N=42$
Age (mean ± SD)	69.5 ± 7.8
PSA in ng/mL (mean ± SD)	12.1 ± 25.1
PET purpose n (%)	
staging	14 (33)
restaging	28 (67)
Previous treatment in restaging group n (%)	
RP	10 (77)
RP + PLND	3 (23)
EBRT	14 (50)
RP + PLND + EBRT	1 (4)
Gleason score n (%)	
6(3 + 3)	5(12)
7(3 + 4)	15(36)
7(4 + 3)	8(19)
8(4 + 4)	4(10)
9(4 + 5)	6(14)
9(5 + 4)	1(2)
10(5 + 5)	3(7)
PET-CT scanner n (%)	
Siemens Biograph mCT	17(40)
Siemens Biograph Vision V600	25(60)
PSMA radioligands	
[^{68}Ga]Ga-PSMA-11	17(40)
[^{18}F]F-PSMA-1007	25(60)
Lymph node spreading n(%)	
Yes	17(40)
No	25(60)
Distant metastases spreading n (%)	
Yes	16(38)
No	26(62)

CT: computed tomography; EBRT: external beam radiotherapy; Liv: Liver; PLND: pelvic lymph node dissection; PET: positron emission tomography; PSA: prostate specific antigen; PSMA-TV: prostate specific membrane antigen-tumor volume; RP, radical prostatectomy

When the entire cohort of patients was split based on their GS Grade Group, i.e., low/intermediate ($GS \leq 7$) and high grade ($GS > 7$), TL-PSMA extracted from [^{18}F] F-PSMA PET images showed significant predictive value for distinguishing between the two Grade Groups (Mann-Whitney test, $p = 0.01$– Fig. 3). The differences in TL-PSMA were even more pronounced when this feature was extracted from PET images of the entire cohort in the combined model, regardless of the PSMA radioligand used (Mann-Whitney test, $p = 0.004$ - Fig. 4). Table 3 provides a list of the most effective conventional and radiomic features for predicting low/intermediate and high GS Grade Group. Conversely, neither TL-PSMA nor other radiomic features significantly differ in the prediction of less/more aggressive disease, when the cohort was divided based on each single GS Grade Group (TL-PSMA with $p = 0.06$, Kruskal-Wallis test).

In the analysis of the prostatic gland/fossa with specific PSMA radioligands, the feature called *Minimum histogram gradient intensity* [16] was identified as a significant predictor of N-status in the combined model (Mann-Whitney test; $p = 0.009$) (Table 4)(Fig. 5).

None of the detected conventional and radiomic features were found to be significantly predictive of distant metastases, both analysing individual PSMA radioligands and the combined model. (Fig. 6)

Discussion

In this study, we present a preliminary investigation that seeks to explore how radiomic analysis from prostatic gland/fossa, derived from [^{68}Ga]Ga-PSMA-11 and [^{18}F] F-PSMA-1007, can be used to predict key clinical outcomes relevant to the staging and restaging of patients with PCa. Main findings of this study are that Prostate TL-PSMA and Intensity-Histogram Gradient-Grey-Level features of different PSMA PET radioligands may predict a high GS and N status in patients with PCa, respectively, while [^{18}F] F-PSMA-1007 -derived TL-PSMA seem to perform better than [^{68}Ga]Ga-PSMA-11 to predict a high GS.

In our experimental configuration, our initial focus was to examine variations between the two PSMA radiopharmaceuticals concerning radiomic features. This investigation aimed to determine whether it was necessary to develop distinct radiomic models for each radioligand or if a combined model could also be considered. The obtained results suggest that the combined model was a valid option, as no statistically significant differences were observed between radiomic variables from the two groups of radiopharmaceuticals (Fig. 1). These results open the possibility of using all the available subjects. Nonetheless, the analysis was extended to both groups singularly in order to assess differences in terms of clinical predictive power in the two groups.

A similar approach was applied to the conventional and radiomic features extracted from the images acquired using different scanners. Again, the results showed that no significant differences were detected between the two groups, suggesting that all the data can be integrated in the same models. These results confirmed our expectations as the scanner used in this study shared similar hardware and settings (Table 1).

No significant correlations between the various examined conventional and radiomic features and the PSA values were found in this study. These findings contrast with the existing literature. For instance, Wang et al. conducted an assessment of the performance of F-PSMA PET radiomics in a group of primary PCa patients, concluding that radiomic signatures

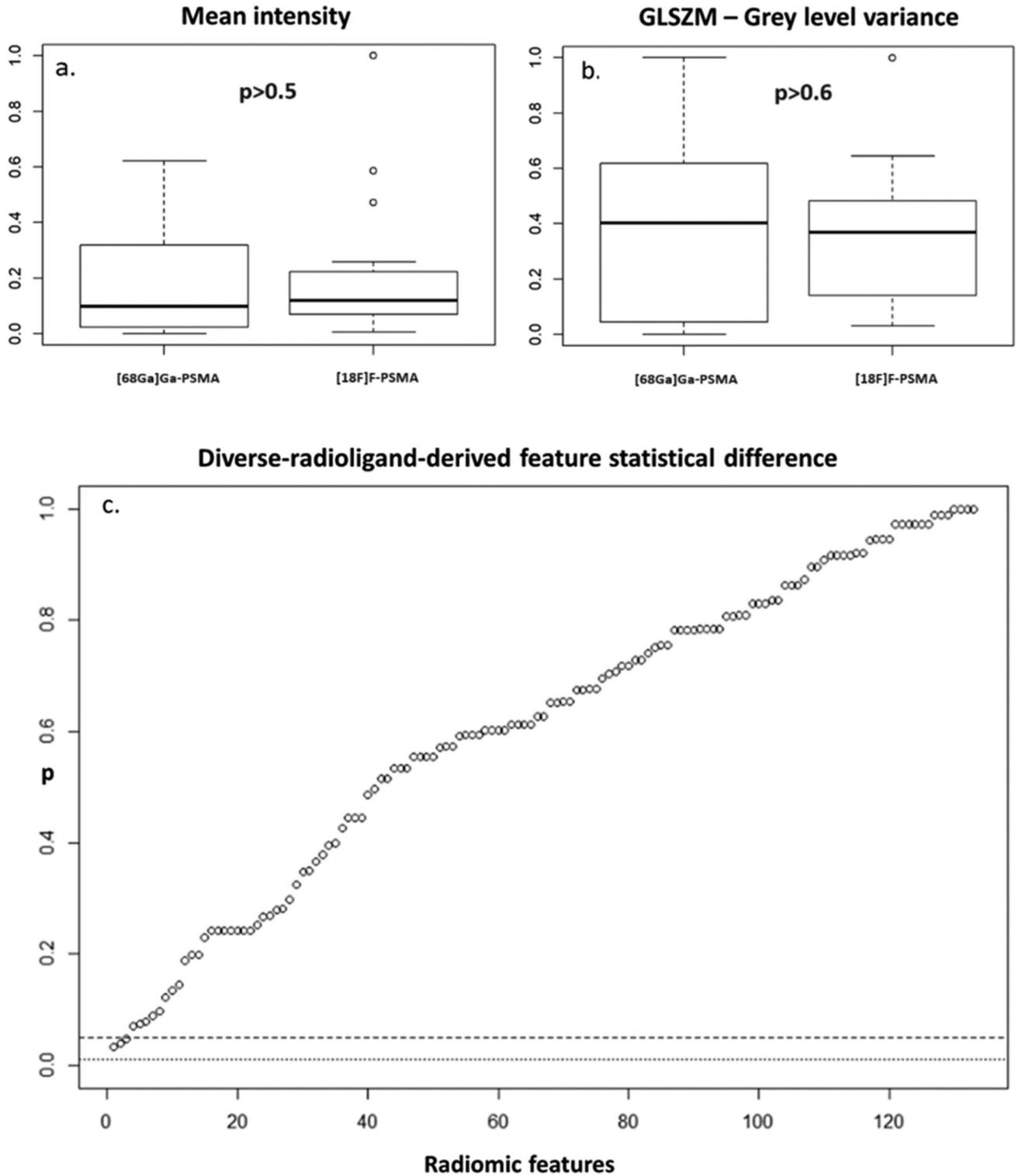

Fig. 1 Radioligands similarity for Radiomic-based comparison purposes. Boxplot graphs of two representative features (**a**, **b**) extracted from PET images with different radioligands (Mean intensity, **a,** GLSZM grey level variance, **b**, showing no significant differences). Graph **c** reports the p-values from the same analysis for all the computed features in ascending order. The dashed and the dotted lines mark respectively the threshold of statistical test significance

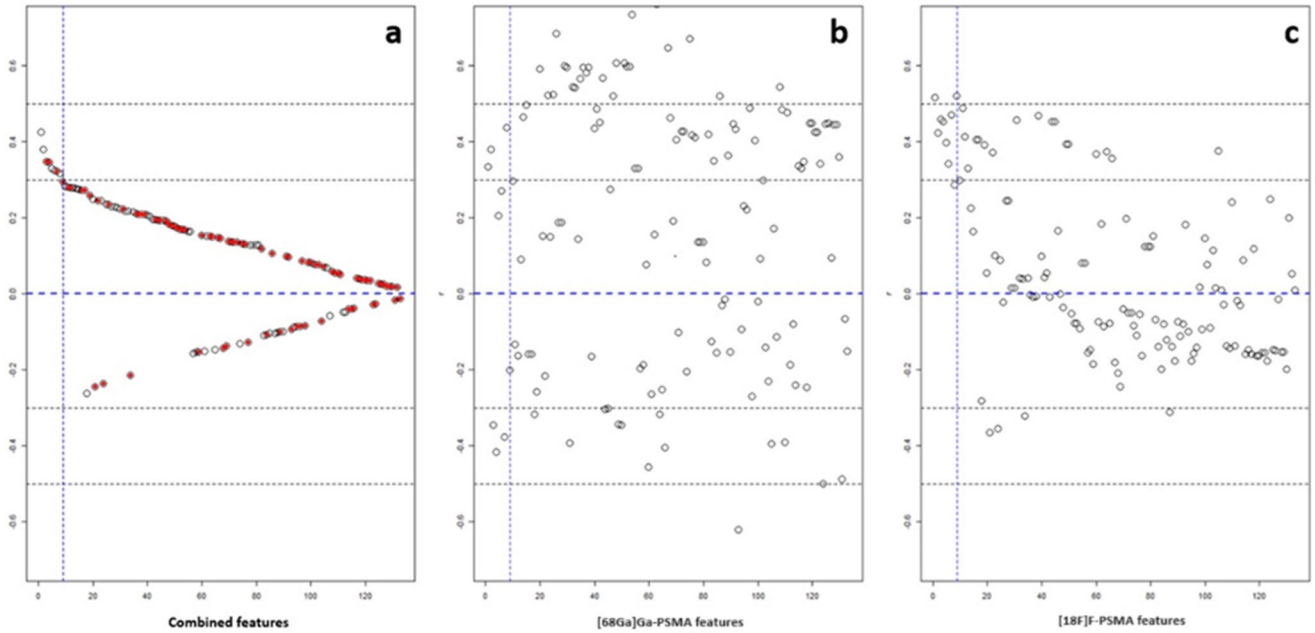

Fig. 2 Radiomic variables and PSA values. Pearson's correlation coefficient (Pearson correlation test among all PCC) (y-axes) and the features (x-axes). The features are ordered according to the decreasing absolute value of the correlation coefficient for (**a**) the entire cohort and separately for (**b**) [^{68}Ga]Ga- PSMA-11 PET and (**c**) [^{18}F]F-PSMA-1007 PSMA PET. The red-marked dots represent the features where the sign of the Pearson index was different, between Gallium and Fluorine cohorts. The horizontal dashed lines, that represent the thresholds to read the strength of the PCC (i.e. absolute(PCC) in [0,0.3] none; absolute(PCC) in [0.3,0.5] weak; absolute(PCC) in [0.5,0.6] moderate; absolute(PCC) > 0.7 high) highlights the absence of significant correlation among radiomic variables and PSA serum values

were effective predictors of PSA levels at staging. Further, the radiomic-based nomogram appeared to have similar predictive performance compared to a clinical nomogram that included PSA levels and GS for risk stratification [17]. The disparities between our findings and those in the existing literature could be attributed, in part, to the relatively small size of our patient cohort as well as to the diverse clinical scenarios in which PSMA PET scans were performed in our study. Namely, the clinical meaning of PSA may vary according to whether a patient is being staged or restaged, as the absolute PSA value alone may not fully reflect the disease burden, particularly during the initial staging, while they appear to be more impactful in the context of restaging. Notably, radiomic features extracted from PSMA PET scans conducted as part of pre-treatment evaluations before Radioligand therapy with [^{177}Lu]Lu-PSMA could predict changes in PSA values, serving as indicators of patient response to treatment [18–20].

PSMA PET metrics proved to be valuable predictors of disease aggressiveness, as reflected by the GS Grade Group. Notably, among these metrics, TL-PSMA from [^{18}F]F-PSMA-1007 PET images emerged as a significant predictor for patients with GS Grade Group ≥ 8. TL-PSMA appears to be a crucial parameter as it combines both the overall in vivo load and the volume of PSMA expression within the PCa tumors. A possible explanation of why this result was found only in the [^{18}F]F-PSMA-1007 group may lie in the distinct distribution characteristics of [^{18}F]F-PSMA-1007 and [^{68}Ga]Ga-PSMA-11. Our analysis primarily focuses on quantitatively assessing PCa lesions within the prostatic gland/fossa. In this context, [^{18}F]F-PSMA-1007 may be better suited for our study's objectives, due to its predominantly hepato-biliary clearance, which simplifies lesion evaluation by minimizing interference from urinary radioactivity in the bladder [21]. Differences of tracer accumulation between the [^{68}Ga]Ga-PSMA-11 and [^{18}F]F-PSMA-1007 are displayed in Fig. 7.

In contrast, neither TL-PSMA nor other radiomic features seem to predicting any single GS Grade Group. These results diverge from the findings reported in the existing literature. For instance, Zamboglou et al. proposed the idea of non-invasively distinguishing between PCa and non-PCa lesions, as well as among PCa lesions with GS of 7 and GS greater than or equal to 8, utilizing specific radiomic features [10]. Similarly, Wang et al. stated that radiomic variables were able to distinguish between low/intermediate and high risk PCa group [17]. Possible causes of the observed discrepancy are the diverse clinical objectives of the PET scans, variations in prior treatments among patients in the restaging subgroup, and the relatively small dataset, even when a combined model was employed.

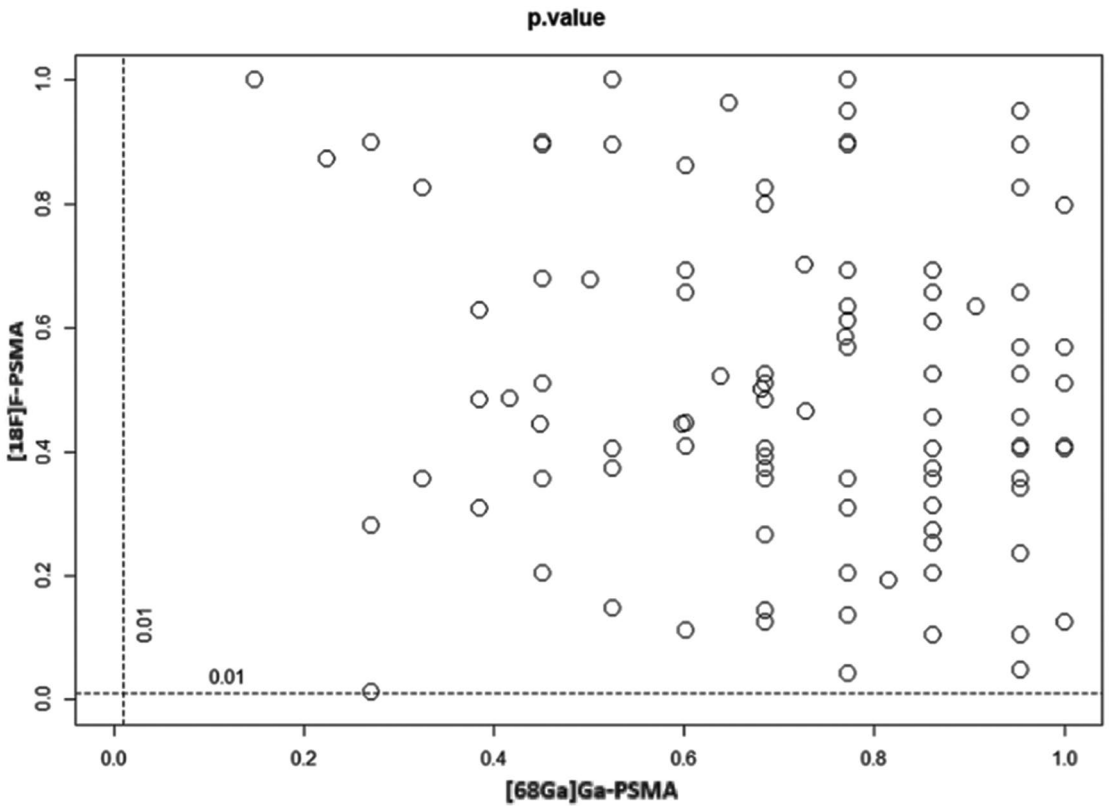

Fig. 3 Radiomic features and dichotomized Gleason score. All radiomic features' predictive value of low/intermediate or high risk PCa extracted from both PSMA radioligands PET images: Each dot represent a feature and the XY- space represents the space of the *p*-values at the Mann-Whitney test for Gallium-labelled and Fluorine-labelled PSMA radioligands, respectively. The dashed lines mark the threshold of 0.01

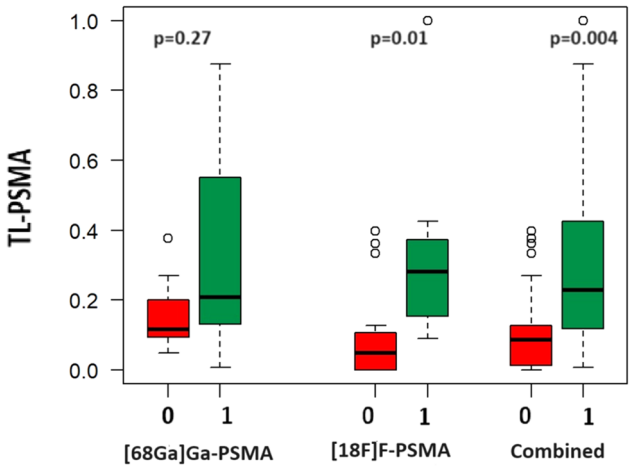

Fig. 4 TL-PSMA and Gleason Score. Box plots graph illustrating the differences of TL-PSMA values between low/intermediate grade (0) and high grade GS (1) subgroups of patients in the Gallium-labelled PSMA cohort, Fluorine-labelled PSMA cohort and in the combined cohort. Differences of TL-PSMA were strongly significant in the combined model ($P=0.004$). Differences of TL-PSMA in the Fluorine cohort were smaller but still significant ($P=0.01$)

Table 3 P-values' rank of 5 best F-PSMA features for predicting low/intermediate and high risk GS PCa

	p-value
TL-PSMA	**0.011**
PSMA-TV	0.044
Strength	0.048
Small zone emphasis	0.104
Normalized zone size-non-uniformity	0.104

P-values in bold reached the statistical significance (Mann Whitney U-test). TL-PSMA, Total lesion PSMA activity; PSMA-TV, PSMA Total Volume

Table 4 P values' rank of 5 radiomic features with best predictive value of lymph node status

	p-value
Minimum histogram gradient intensity	**0.009**
Busyness	0.042
Long runs emphasis	0.063
Run percentage	0.063
Inverse difference	0.074

P-values in bold reached the statistical significance (Mann Whitney U-test)

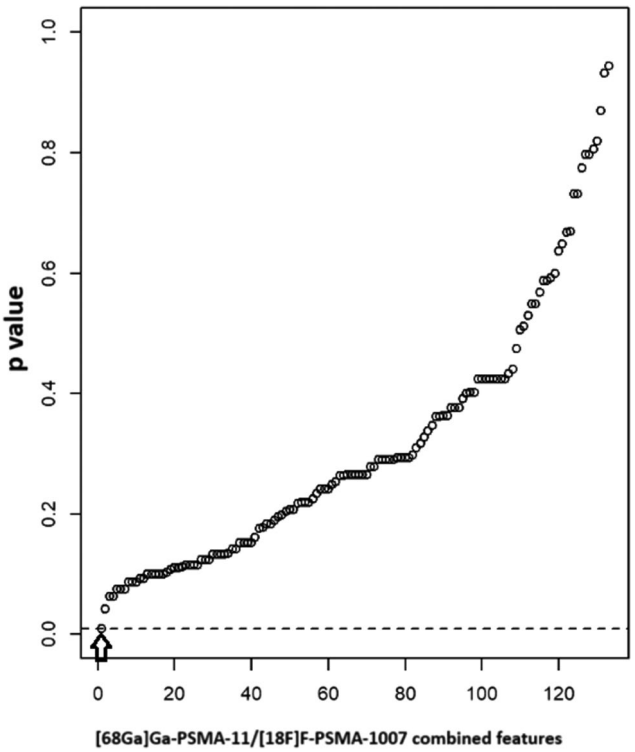

Fig. 5 Radiomic features and lymph node status. The position of the radiomic features's *p*-values (y-axis) extracted from both [^{68}Ga]Ga-PSMA-11 and [^{18}F]F-PSMA-1007 (x-axis) at the Mann-Whitney tests, for prediction of lymph node status. *Minimum Histogram Gradient Intensity* (arrow) reached the set statistical significance

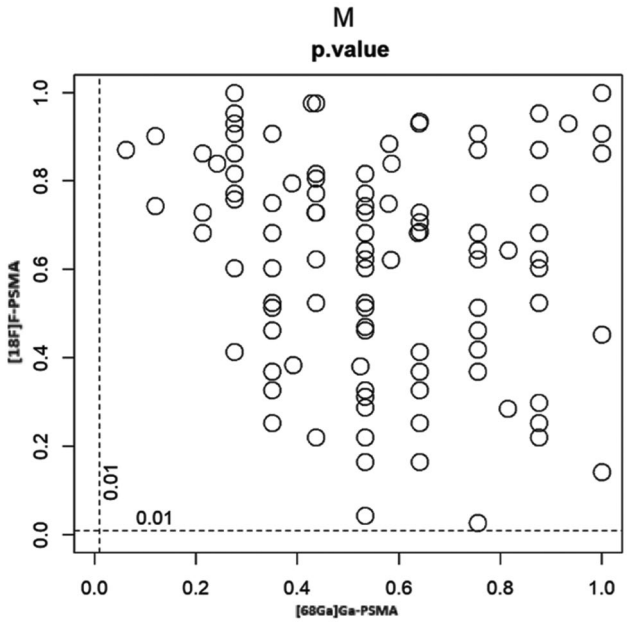

Fig. 6 Radiomic Features and presence of distant metastases. The position of the radiomic features's *p*-values extracted from gallium-labelled PSMA radioligands (x-axis) vs. fluorine-labelled PSMA radioligands (y-axis) at the Mann-Whitney tests, for prediction of metastatic spreading of disease (M). None of them reach the set statistical significance

The abovementioned authors documented a strong correlation between radiomic features and the presence of histologically-confirmed lymph node metastases [10, 17]. These results are in line with our data. Notably, the *Minimum histogram gradient intensity* was found to be significant predictor of N-status. These results were somehow anticipated, considering that lymph node metastases are a characteristic manifestation of tumor aggressiveness, similar to a high GS.

Unlike previously reported results [22], none of the features computed from prostatic gland/fossa in this study was found significantly able to predict the presence of distant metastases. Nevertheless, the ability of radiomic features to forecast the presence or timing of metastasis through PET imaging remains uncertain, and it appears to be influenced by various factors, including the specific organ being examined [23–25].

Some limitations warrant consideration. These include the retrospective nature of our investigations, which entailed a lack of histological and clinical data during follow-up, the diverse clinical objectives of patients undergoing [^{68}Ga]Ga-PSMA-11 and [^{18}F]F-PSMA-1007 PET and the relatively small sample size in our study. Moreover, the small cohort prevented us to perform further subgroup's analyses, aimed to display how radiomic features from each radiopharmaceuticals behave within both staging and restaging subgroups. Larger cohort's studies should be crucial to explore the performance of PSMA-derived radiomic features according to the diverse clinical scenarios and PET purposes. In addition, while the absence of an independent validation cohort is somewhat anticipated in pilot and small cohort studies [26–30], it should be acknowledged as another limitation. Such validation would enhance the robustness of our model in terms of generalizability to other datasets.

Conclusion

In this comparative study, TL-PSMA and the *Minimum histogram gradient intensity* features from prostatic gland/fossa PET images of the [^{68}Ga]Ga-PSMA-11 and [^{18}F]F-PSMA-1007 radioligands seem to non-invasively predict both high GS and N-status in PCa patients. Prospective studies with independent validation cohort are warranted to confirm these preliminary data and to explore about the potential inclusion of a radiomic model in the clinical nomogram of PCa patients.

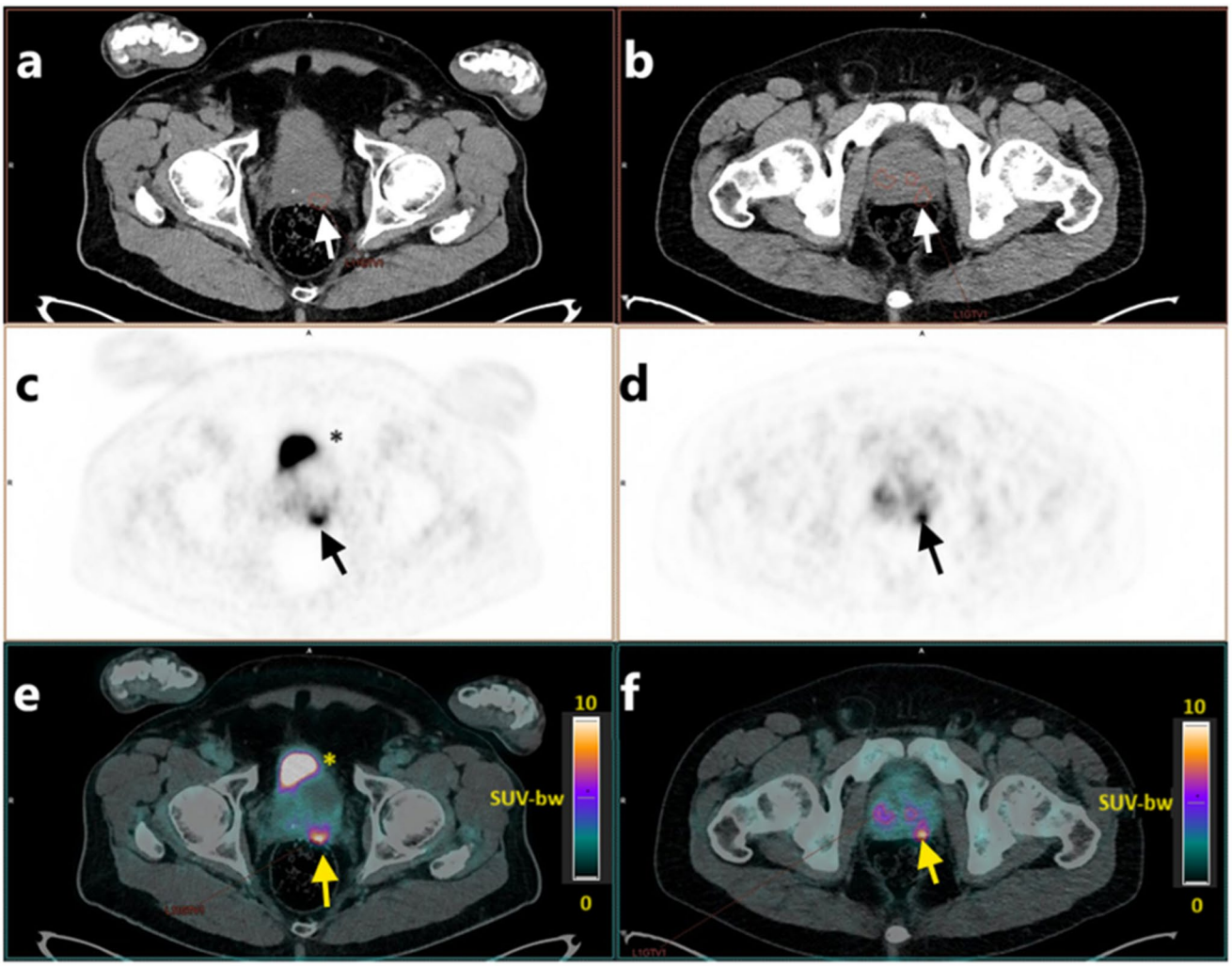

Fig. 7 Two pictorial cases of [^{68}Ga]Ga-PSMA-11 and [^{18}F]F-PSMA-1007 PET/CT in PCa patients for primary staging. VOIs of PET images were propagated on corresponding CT images (a, b) to create RT structures (arrows), as basis for radiomic features' extraction. VOIs had been previously placed to contour primary PCa lesions located in left prostate lobes (arrows), according to PET images only (c, d) and PET fused images (e, f). VOIs isocount might be hampered by physiologic accumulation of [^{68}Ga]Ga-PSMA-11 in the bladder (asterisk)

Acknowledgements A special thanks to Fondazione Umberto Veronesi (FUV). Daniele Antonio Pizzuto won the post-doctoral fellowship FUV 2023 to be financially supported for the application of radiomics in patients with prostate cancer. A special thanks to all colleagues (costumer service, nurses, technicians, physicians) working at the centro PET-TC of Fondazione Policlinico Universitario A. Gemelli IRCCS for ensuring high volumes and high standards of quality of PET images every day.

Author contributions Authors D.A.P, C.Z, L.B., R.G., M.D.S., M.G., M.R.R., C.C., S.A. contributed for all following aspects: (a) "conception and design, or acquisition of data, or analysis and interpretation of data," (b) "drafting the article or revising it critically for important intellectual content," (c) "final approval of the version to be published," and (d) "agreement to be accountable for all aspects of the work in ensuring that questions related to the accuracy or integrity of any part of the work are appropriately investigated and resolved."Particularly D.A.P and S.A. focused on "(a), (b) (c) and (d) points. C.Z. and C.C. mainly focused on (b), (c) and (d), L.B. mainly focused on (c) and (d). R.B. and M.G. mainly focused on (a) and (d), M.D.S. mainly focused on (a) and (d). M.R.R. focused on (a), (c), (d).

Data availability No datasets were generated or analysed during the current study.

Declarations

Competing interests The authors declare no competing interests.

Conflicts of interest disclosure Authors do not declare any conflicts of interest on the topic of this study.

References

1. Herlemann A, Wenter V, Kretschmer A et al (2016) 68Ga-PSMA Positron Emission Tomography/Computed Tomography provides

Accurate Staging of Lymph Node regions prior to Lymph Node Dissection in patients with prostate Cancer. Eur Urol 70:553–557
2. Bouchelouche K, Choyke PL (2018) Advances in prostate-specific membrane antigen PET of prostate cancer. Curr Opin Oncol 30:189–196
3. Afshar-Oromieh A, Avtzi E, Giesel FL et al (2015) The diagnostic value of PET/CT imaging with the 68Ga-labelled PSMA ligand HBED-CC in the diagnosis of recurrent prostate cancer. Eur J Nucl Med Mol Imaging 42:197–209
4. Grubmüller B, Baltzer P, Hartenbach S et al (2018) PSMA Ligand PET/MRI for primary prostate Cancer: staging performance and clinical impact. Clin Cancer Res 24:6300–6307
5. Sonni I, Felker ER, Lenis AT et al (2022) Head-to-Head comparison of ^{68} Ga-PSMA-11 PET/CT and mpMRI with a Histopathology Gold Standard in the detection, Intraprostatic Localization, and determination of local extension of primary prostate Cancer: results from a prospective single-center imaging trial. J Nucl Med 63:847–854
6. Fendler WP, Calais J, Eiber M et al (2019) Assessment of ^{68} Ga-PSMA-11 PET accuracy in localizing recurrent prostate Cancer: a prospective single-arm clinical trial. JAMA Oncol 5:856
7. Afshar-Oromieh A, Zechmann CM, Malcher A et al (2014) Comparison of PET imaging with a 68Ga-labelled PSMA ligand and 18F-choline-based PET/CT for the diagnosis of recurrent prostate cancer. Eur J Nucl Med Mol Imaging 41:11–20
8. Kuten J, Fahoum I, Savin Z et al (2020) Head-to-Head comparison of ^{68} Ga-PSMA-11 with ^{18} F-PSMA-1007 PET/CT in staging prostate Cancer using histopathology and Immunohistochemical Analysis as a reference Standard. J Nucl Med 61:527–532
9. Hoffmann MA, Von Eyben FE, Fischer N et al (2022) Comparison of [18F]PSMA-1007 with [68Ga]Ga-PSMA-11 PET/CT in restaging of prostate Cancer patients with PSA Relapse. Cancers 14:1479
10. Zamboglou C, Carles M, Fechter T et al (2019) Radiomic features from PSMA PET for non-invasive intraprostatic tumor discrimination and characterization in patients with intermediate- and high-risk prostate cancer - a comparison study with histology reference. Theranostics 9:2595–2605
11. Spohn SKB, Schmidt-Hegemann N-S, Ruf J et al (2023) Development of PSMA-PET-guided CT-based radiomic signature to predict biochemical recurrence after salvage radiotherapy. Eur J Nucl Med Mol Imaging 50:2537–2547
12. Mottet N, van den Bergh RCN, Briers E et al (2021) EAU-EANM-ESTRO-ESUR-SIOG guidelines on prostate Cancer—2020 update. Part 1: screening, diagnosis, and local treatment with curative intent. Eur Urol 79:243–262
13. Ceci F, Oprea-Lager DE, Emmett L et al (2021) E-PSMA: the EANM standardized reporting guidelines v1.0 for PSMA-PET. Eur J Nucl Med Mol Imaging 48:1626–1638
14. Boellaard R, Delgado-Bolton R, Oyen WJG et al (2015) FDG PET/CT: EANM procedure guidelines for tumour imaging: version 2.0. Eur J Nucl Med Mol Imaging 42:328–354
15. Nioche C, Orlhac F, Boughdad S et al (2018) LIFEx: a freeware for Radiomic feature calculation in Multimodality Imaging to accelerate advances in the characterization of Tumor Heterogeneity. Cancer Res 78:4786–4789
16. Zwanenburg A, Vallières M, Abdalah MA et al (2020) The image Biomarker Standardization Initiative: standardized quantitative Radiomics for High-Throughput Image-based phenotyping. Radiology 295:328–338
17. Wang Z, Li Y, Zheng A et al (2022) Evaluation of a radiomics nomogram derived from Fluoride-18 PSMA-1007 PET/CT for risk stratification in newly diagnosed prostate cancer. Front Oncol 12:1018833
18. Roll W, Schindler P, Masthoff M et al (2021) Evaluation of 68Ga-PSMA-11 PET-MRI in patients with advanced prostate Cancer receiving 177Lu-PSMA-617 therapy: a Radiomics Analysis. Cancers 13:3849
19. Assadi M, Manafi-Farid R, Jafari E et al (2022) Predictive and prognostic potential of pretreatment 68Ga-PSMA PET tumor heterogeneity index in patients with metastatic castration-resistant prostate cancer treated with 177Lu-PSMA. Front Oncol 12:1066926
20. Khurshid Z, Ahmadzadehfar H, Gaertner FC et al (2018) Role of textural heterogeneity parameters in patient selection for 177Lu-PSMA therapy via response prediction. Oncotarget 9:33312–33321
21. Sanchez-Crespo A (2013) Comparison of Gallium-68 and Fluorine-18 imaging characteristics in positron emission tomography. Appl Radiat Isot 76:55–62
22. Cysouw MCF, Jansen BHE, van de Brug T et al (2021) Machine learning-based analysis of [(18)F]DCFPyL PET radiomics for risk stratification in primary prostate cancer. Eur J Nucl Med Mol Imaging 48:340–349
23. Peng L, Hong X, Yuan Q, Lu L, Wang Q, Chen W (2021) Prediction of local recurrence and distant metastasis using radiomics analysis of pretreatment nasopharyngeal [18F]FDG PET/CT images. Ann Nucl Med 35:458–468
24. Gao J, Bai Y, Miao F et al (2023) Prediction of synchronous distant metastasis of primary pancreatic ductal adenocarcinoma using the radiomics features derived from 18F-FDG PET and MRI. Clin Radiol 78:746–754
25. Pullen LCE, Noortman WA, Triemstra L et al (2023) Prognostic value of [18F]FDG PET Radiomics to detect peritoneal and distant metastases in locally advanced gastric Cancer—A side study of the prospective multicentre PLASTIC study. Cancers 15:2874
26. Amorim BJ, Torrado-Carvajal A, Esfahani SA et al (2020) PET/MRI radiomics in rectal Cancer: a pilot study on the correlation between PET- and MRI-Derived image features with a clinical interpretation. Mol Imaging Biology 22:1438–1445
27. Esfahani SA, Torrado-Carvajal A, Amorim BJ et al (2022) PET/MRI and PET/CT Radiomics in primary cervical Cancer: a pilot study on the correlation of pelvic PET, MRI, and CT derived image features. Mol Imaging Biology 24:60–69
28. Chen Y-H, Lue K-H, Chu S-C et al (2019) Combining the radiomic features and traditional parameters of 18F-FDG PET with clinical profiles to improve prognostic stratification in patients with esophageal squamous cell carcinoma treated with neoadjuvant chemoradiotherapy and surgery. Ann Nucl Med 33:657–670
29. Negreros-Osuna AA, Parakh A, Corcoran RB et al (2020) Radiomics texture features in Advanced Colorectal Cancer: correlation with *BRAF* Mutation and 5-year overall survival. Radiology: Imaging Cancer 2:e190084
30. Subhawong TK, Feister K, Sweet K et al (2021) MRI volumetrics and image texture analysis in assessing systemic treatment response in Extra-abdominal Desmoid Fibromatosis. Radiology: Imaging Cancer 3:e210016